



Article

Alkali Iodide Deep Eutectic Solvents as Alternative Electrolytes for Dye Sensitized Solar Cells

Hugo Cruz ^{*,†}, Ana Lucia Pinto [†] , Noémi Jordão, Luísa A. Neves  and Luís C. Branco ^{*}

LAQV-REQUIMTE, Departamento de Química, Faculdade de Ciências e Tecnologia, Universidade Nova de Lisboa, 2829-516 Caparica, Portugal; al.pinto@campus.fct.unl.pt (A.L.P.); n.jordao@fct.unl.pt (N.J.); luisa.neves@fct.unl.pt (L.A.N.)

* Correspondence: hg.cruz@fct.unl.pt (H.C.); l.branco@fct.unl.pt (L.C.B.)

† Same contribution from both authors.

Abstract: Different alkali deep eutectic solvents (DES), such as LiI:nEG, NaI:nEG, and KI:nEG, have been tested as electrolytes for dye sensitized solar cells (DSSCs). These DSSCs were prepared using pure DES or, alternatively, DES combined with different amounts of iodine (I₂). The most important parameters, such as open circuit voltage (V_{OC}), short circuit current density (J_{SC}), fill factor (FF), and the overall conversion efficiency (η), were evaluated. Some DES seem to be promising candidates for DSSC applications, since they present higher V_{OC} (up to 140 mV), similar FF values but less current density values, when compared with a reference electrolyte in the same experimental conditions. Additionally, electrochemical impedance spectroscopy (EIS) has been performed to elucidate the charge transfer and transport processes that occur in DSSCs. The values of different resistance (Ω·cm²) phenomena and recombination/relaxation time (s) for each process have been calculated. The best-performance was obtained for DES-based electrolyte, KI:EG (containing 0.5 mol% I₂) showing an efficiency of 2.3%. The efficiency of this DES-based electrolyte is comparable to other literature systems, but the device stability is higher (only after seven months the performance of the device drop to 60%).

Keywords: deep eutectic solvents (DES); electrolytes; dye sensitized solar cells (DSSC)



Citation: Cruz, H.; Pinto, A.L.; Jordão, N.; Neves, L.A.; Branco, L.C. Alkali Iodide Deep Eutectic Solvents as Alternative Electrolytes for Dye Sensitized Solar Cells. *Sustain. Chem.* **2021**, *2*, 222–236. <https://doi.org/10.3390/suschem2020013>

Academic Editors: Matthew Jones, Ana B. Pereiro and João M. M. Araújo

Received: 31 December 2020

Accepted: 22 March 2021

Published: 6 April 2021

Publisher's Note: MDPI stays neutral with regard to jurisdictional claims in published maps and institutional affiliations.



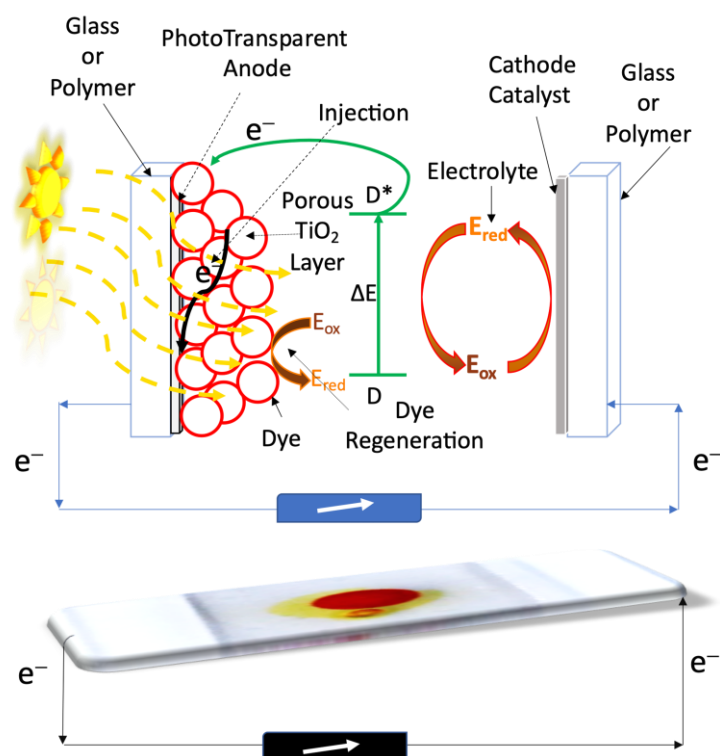
Copyright: © 2021 by the authors. Licensee MDPI, Basel, Switzerland. This article is an open access article distributed under the terms and conditions of the Creative Commons Attribution (CC BY) license (<https://creativecommons.org/licenses/by/4.0/>).

1. Introduction

In the past few years, the design of alternative and renewable energy technologies has been considered to be one of the current and most important challenges due to the growth in the energy requirement by the world population demands. Ref. [1] In this context, one of the most promising energy sources to efficiently generate energy is harvested from the sun, which can be considered as an abundant, clean, safe resource, and with higher economic value, particularly for remote areas. Ref. [2] Currently, solar energy and its conversion into electricity received much attention and, consequently, its production is increasing over the years. The conventional solar cell is the silicon-based cell with 15 to 25% of efficiency, but possessing high costs and requiring a larger photoactive area. Ref. [3] Brian O'Regan and Michael Grätzel [4] introduced Dye-Sensitized Solar Cells (DSSC) as photovoltaic devices based on the sensitization of wide band-gap semiconductor electrodes with dyes absorbing visible light. The production of electrical energy is achieved as electrons flow from the photoexcited dye toward the semiconductor. Electrons are then transported through the mesoporous TiO₂ electrode to the cathode through an external circuit, and, finally, used for the reduction of the electrolyte used to re-establish the original state of the dye [5] (see Scheme 1).

These devices received much attention, since they display a large flexibility in shape, colour, and transparency, as well as compatibility with flexible substrates, which allows a large variety of designs to facilitate market entry [4,6,7]. Different dyes have been applied in DSSCs, such as ruthenium dyes [8,9] (possessing low availability and high cost associated

to the ruthenium), porphyrins [10–12], anthocyanins [13–18], and, more recently, quantum dots [19] and perovskites [20–22].



Scheme 1. Illustration of a Dye Sensitized Solar Cell (DSSC) with the main components (Working Principles).

The development of new sensitizers for DSSCs is a hot topic of research in order to improve the overall efficiency of the cell as well as to reduce the production costs. Furthermore, the photo-anode (PA) and cathode (counter electrode, CE), as well as the electrolyte, are also important components in order to obtain higher overall DSSC performance. Indeed, the electrolyte plays a relevant role in completing the circuit by assuring charge transport between the PA and CE, thus allowing dye regeneration, but its selection is one of the major drawbacks in DSSCs. As electrolytes, it is common to use organic volatile solvents (e.g., acetonitrile). Moreover, mixtures of solvents are often included to decrease electrolyte volatility, since, during the cell lifetime, electrolyte evaporation can occur and, thus, the leakage of the cell, negatively affecting the overall performance of the device, mainly its stability over time.

Different systems have been explored to overcome this drawback, such as water-based [23], quasi-solid [24], or solid [25] electrolytes, but some limitations that are related to lower power energy conversion have been reported [23–25]. In this context, Deep Eutectic Solvents (DES), which can be comparable to room temperature ionic liquids (RTILs), became a promising alternative electrolyte for electrochemical applications. Ref. [26] Usually, DES are obtained by a suitable combination between hydrogen-bond acceptors (HBA) and hydrogen-bond donors (HBD). Refs. [27,28] In general, DES exhibit much of the peculiar properties of RTILs, but they are easier to prepare with high purity and while using low-cost starting materials. Refs. [27,28] In the last years, DES are defined as green solvents for a large range of potential applications: (i) electroplating and electrodeposition processes [29,30]; (ii) electrocatalysis and for super-capacitors or batteries [31–35]; (iii) alternative media to organic synthesis [36], including in preparation and stabilization of Metal-Organic Frameworks (MOFs) [37,38]; and, (iv) low-cost and alternative electrolytes for electrochromic devices [39–41], acting simultaneously as electrochromic and electrolyte [42], among others.

In last years, few examples of DES as electrolytes for solar cells have been reported:

- (1) the first one, comprises an aqueous electrolyte (15 wt%) based on choline iodide and glycerol (ChI:Gly) as eutectic mixture (solid at room temperature) as part of the electrolyte composition for DSSCs. Ref. [43] The reported electrolyte contains 0.2 M of iodine (I_2), 0.5 M of N-methylbenzimidazole in a mixture of 1-propyl-3-methylimidazolium iodide ([PMIM]I) and the prepared binary mixture (*v/v*, 13:7). The selected sensitizer dye was the metal-free indoline dye D149, because it is more suitably mixed with the highly viscous electrolyte. The reported DSSCs showed an open circuit voltage (V_{OC}) of 0.533 V, short circuit current density (J_{sc}) of $12.0 \text{ mA}\cdot\text{cm}^{-2}$, a fill factor of 0.582 and 3.88% of energy conversion efficiency under AM 1.5, $100 \text{ mW}/\text{cm}^2$ illuminations [43];
- (2) a similar approach using an aqueous electrolyte (40% *w/w* water content) that was composed by choline chloride and glycerol eutectic mixtures (ChCl/Gly, 1:2 mol/mol) as an effective electrolyte solvent for DSSCs have been reported. Ref. [44] The selected sensitizer dye corresponds to the hydrophilic PTZ-TEG dye. The authors reported that the best DSSCs performance was obtained using a 2 M of 1-propyl-3-methylimidazolium iodide ([PMIM]I), 0.1 M of guanidinium thiocyanate (GuSCN) in a 40% aqueous solution of ChCl:Gly. In this case, the DSSCs showed V_{OC} of 0.504 V, J_{SC} of $5.1 \text{ mA}\cdot\text{cm}^{-2}$, FF of 0.66, and an overall power conversion efficiency (PCE) of 1.7%;
- (3) later, the same authors reported a hydrophobic eutectic solvent composed by DL-menthol and acetic acid as an eco-friendly passive electrolyte medium for DSSCs [45]; and,
- (4) more recently, natural deep eutectic solvents (NADES) as effective electrolyte solutions for DSSCs have been also reported. Ref. [46] These aqueous (20–30 wt%) NADES are composed by sugars (e.g., Glucose, Sorbitol, Fructose, and mannose) and choline chloride (ChCl). The authors investigated the potential active involvement of DES media with a selected phenothiazine-based sensitizer, which is composed by a glucose functionality, and a glucose based-co-adsorbent (glucuronic acid) to improve the photovoltaic performance. The reported electrolyte was composed by iodine (20 mM), 2 M [PMIM]I in different aqueous NADESs.

Herein, different Deep Eutectic Solvents that are composed by lithium, sodium, or potassium iodide salts, as HBAs combined with glycerol (Gly), ethylene glycol (EG), and poly(ethylene glycol) ($M_w = 200, 400 \text{ g/mol}$) as HBDs have been developed (see Figure 1). In this work, some representative eutectic systems based on alkali iodides were incorporated in DSSCs to evaluate their overall energy efficiency and performance as sustainable electrolytes.

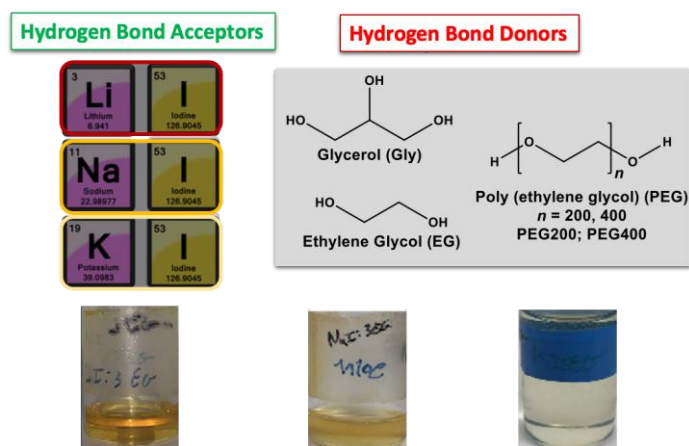


Figure 1. Chemical Structures of Hydrogen Bond Acceptors (HBA) and Donors (HBD) selected for the preparation of alkali iodide Deep Eutectic Solvents.

2. Results and Discussion

The reported eutectic mixtures are promising electrolytes for energy application due to the higher iodide content in its composition. Thus, the DSSCs were fabricated using the following configuration: an anode with a nanocrystalline TiO₂ film, a sensitizer dye ruthenium tris(2,2'-bipyridine) derivative (N719), adsorbed to the TiO₂, and, finally, a Pt counter-electrode. The cell assembly is based on the sandwich type of architecture, and the electrolyte is later injected through a hole that was previously made in the cathode.

Different parameters should be evaluated to evaluate the DES ability to act as intrinsically electrolytes for DSSCs: (i) open circuit voltage (V_{OC}); (ii) short circuit current density (J_{SC}); and, (iii) fill factor (FF) and the overall conversion efficiency (η) were measured under AM 1.5 solar light ($100 \text{ mW} \cdot \text{cm}^{-2}$). Firstly, LiI:3EG, NaI:3EG, KI:5EG, and LiI:10EG were tested as electrolytes, confirming that, in the absence of I₂, the efficiency is close to zero. Table 1 summarizes the results after the addition of iodine (I₂) to the eutectic mixtures and Figure 2 shows the photocurrent–voltage (J–V) plot.

Table 1. Photovoltaic performance parameters of DSSCs based on dye N719 for the different alkali eutectic mixtures as electrolyte, under $100 \text{ mW} \cdot \text{cm}^{-2}$ simulated AM 1.5 illumination. (The results presented are for the best performing cell).

Electrolyte	V_{OC} (mV)	J_{SC} (mA/cm ²)	V_{max} (mV)	J_{max} (mA/cm ²)	FF	η (%)
LiI:3EG (plus 1 mol% I ₂)	457	4.00	346	3.21	0.60	1.12
NaI:3EG (plus 1 mol% I ₂)	460	4.05	347	3.32	0.62	1.16
KI:5EG (plus 0.1 mol% I ₂)	543	2.07	467	1.63	0.67	0.77
KI:5EG (plus 0.5 mol% I ₂)	545	6.05	433	5.26	0.69	2.30
KI:5EG (plus 1 mol% I ₂)	483	4.42	356	3.52	0.59	1.27
KI:5EG (plus 2.5 mol% I ₂)	493	3.86	367	3.06	0.59	1.14
KI:5EG (plus 10 mol% I ₂)	51	0.13	26	0.05	0.27	0.00
LiI:10EG (plus 0.5 mol% I ₂)	572	4.50	446	3.57	0.62	1.61
LiI:10EG (plus 1 mol% I ₂)	560	4.42	427	3.57	0.62	1.55

The eutectic mixtures LiI:nEG, NaI:nEG, and KI:nEG (plus 1 mol% of I₂) presented open circuit voltage results (V_{OC}) of 457 mV, 460 mV, and 483 mV, respectively. In general, despite the lower concentration of I₂ compared to the reference electrolyte, in the same experimental conditions, the obtained V_{OC} values are higher than the value that is obtained for the reference, which is 431 mV. Furthermore, the increase of the cation size from Li⁺ to K⁺ provoked an increase in the open circuit voltage results. Upon photoexcitation, injected electrons accumulate in the semiconductor conduction band, and the cations in the electrolyte intercalate in the mesoporous film for charge compensation. Refs. [47,48] The small-sized Li⁺ is easily adsorbed onto the film surface than the K⁺. The intercalation of Li⁺ suggested a positive movement of the TiO₂ flat band potential, thus decreasing the V_{OC} of the device when compared with the V_{OC} that was obtained for the K⁺. A consequent increase in the driving force for electron injection from the dye to TiO₂ is expected, favouring J_{SC} over V_{OC} , according to the positive shift in the TiO₂ Fermi level.

In parallel, the increase in cation size provoked an increase in J_{SC} resulting in higher efficiencies for the KI:EG-based electrolyte.

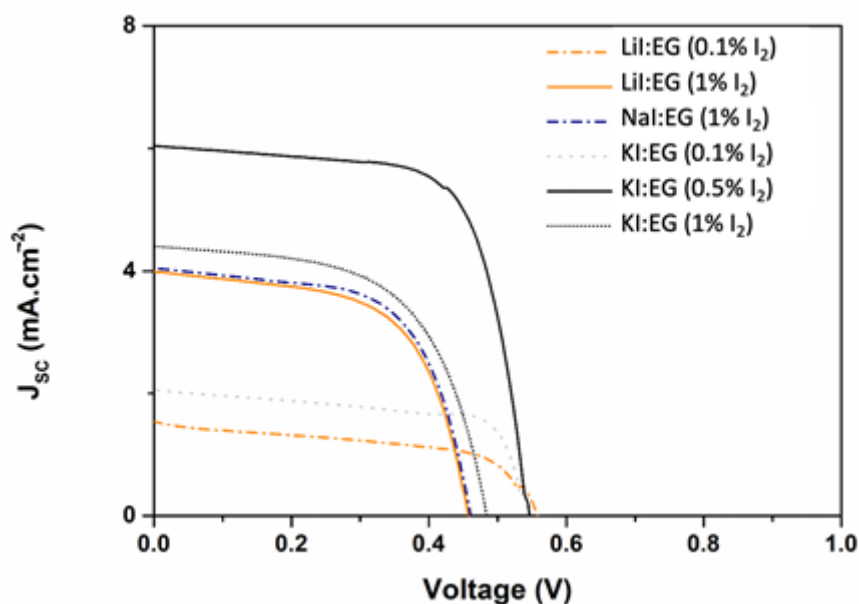


Figure 2. Photocurrent–voltage (J–V) curves of DSSCs based on dye N719 for the different alkali eutectic mixtures as electrolyte under $100 \text{ mW}\cdot\text{cm}^{-2}$ simulated AM 1.5 illumination (for all prepared alkali eutectic mixtures with different mol% of iodine).

Increasing the amount of I_2 is expected to reflect in a higher cell performance (for example the commercial reference electrolyte contains 10 mol% I_2). For the KI:5EG-based electrolyte, different concentrations of I_2 from 0.1 to 10 mol% were tested and the results are presented in Table 1. From 0.1 to 0.5 mol% I_2 , there is an overall increase in cell efficiency from 0.77 to 2.30%, mainly due to an increase in the photocurrent produced (~3-fold higher for the 0.5 mol% I_2). However, increasing the amount of I_2 from 0.5 mol% to 1, 2.5, and 10 mol% corresponds in a decrease in all cell parameters, resulting in lower efficiencies (reaching 0% efficiency for KI:5EG + 10 mol% I_2). These results can be related to bigger electron recombination due to an increase in tri-iodide concentration near the semiconductor. Furthermore, the colour of the electrolytes has a major effect in the obtained results. In the case of the KI:5EG + 10 mol% I_2 , the results can be justified by the dark-brown coloration of the electrolyte. One of the drawbacks of electrolytes based on the I^-/I_3^- redox couple is that a significant portion of the visible light is screened from the sensitized TiO_2 film due to the absorption of I_3^- . Ref. [48] This effect is so accentuated that the electrolyte might be screening all of the irradiated light, therefore no photoexcitation of the dye occurs; hence, no electron injection is verified, and no efficiency is obtained.

Increasing EG concentration is expected to decrease the electrolyte viscosity [39,40], thus increasing device performance due to facilitated mass and electron transport. We also studied the influence of a 3.3-fold increase in EG concentration for the Li-based DES (Table 1; Li:3EG + 1 mol% I_2 and Li:10EG + 1 mol% I_2). In the case of Li:10EG + 1 mol% I_2 , it is important to note that the significant increase in V_{OC} (100 mV) is in agreement with higher EG concentration showing an overall efficiency of 1.55%.

In general, the prepared DSSCs using the alkali DES as electrolyte revealed that the lower conversion efficiency mainly arises from the lower photocurrent. This result can be explained by a slower charge and mass transport through the electrolyte, leading to lower currents. The fill factor parameter presents a similar behaviour in all tested electrolytes.

The best results were obtained for 0.5 mol% of I_2 added to the electrolyte. Further optimization of eutectic mixture composition should be performed in order to increase its potential as a non-volatile and non-flammable, with reduced amounts of additional I_2 , to

increase the overall performance of DSSCs. A very promising property of the use of DESs is the performance lifetime of the DSSCs.

From Figure 3, it is possible to observe that the DSSC based on the alkali DES KI:5EG + 0.5 mol% I₂ as electrolyte still works after one-month of operation, a decrease of around 50% of its efficiency is observed. After seven months, it is still working, but with a further decrease in performance by over 60%. These results were obtained with the same cell, with no addition of fresh electrolyte or dye. This represents an improvement when comparing to reference cells, where after one month, does not work due to electrolyte evaporation.

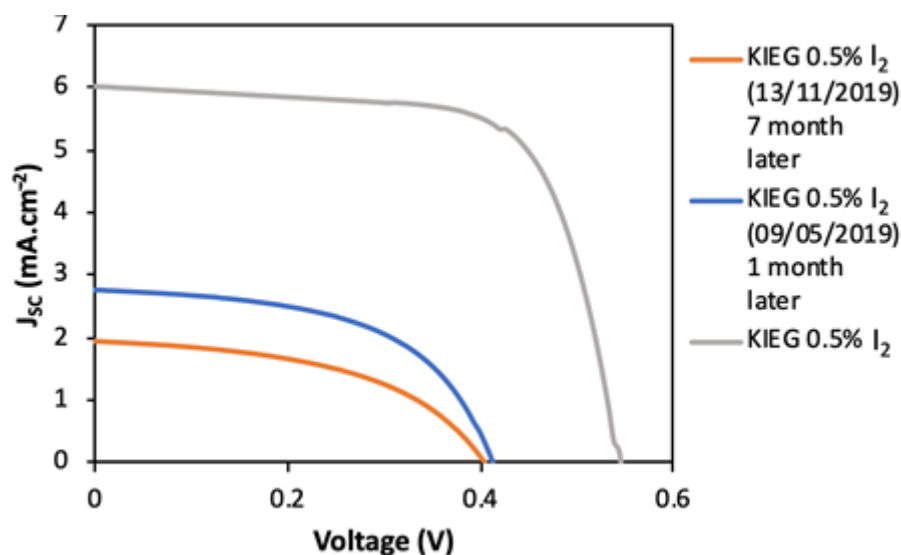


Figure 3. J–V curves of DSSCs based on dye N719 for the alkali DES KI:EG as electrolyte, under 100 mW·cm^{−2} simulated AM 1.5 illumination: describing the decrease of the performance of the cell over time.

Additionally, electrochemical impedance spectroscopy was performed to elucidate about the charge transfer (electronic process) and transport (ionic) processes in the prepared DSSCs [9].

The signal inputted is a small sinusoidal voltage stimulus of a fixed frequency that is applied to an electrochemical cell and its current response is measured [9]. The behaviour of an electrochemical system, in this first case, the electrolyte iodide based-DES, can be investigated by sweeping the frequency over several orders of magnitude [9].

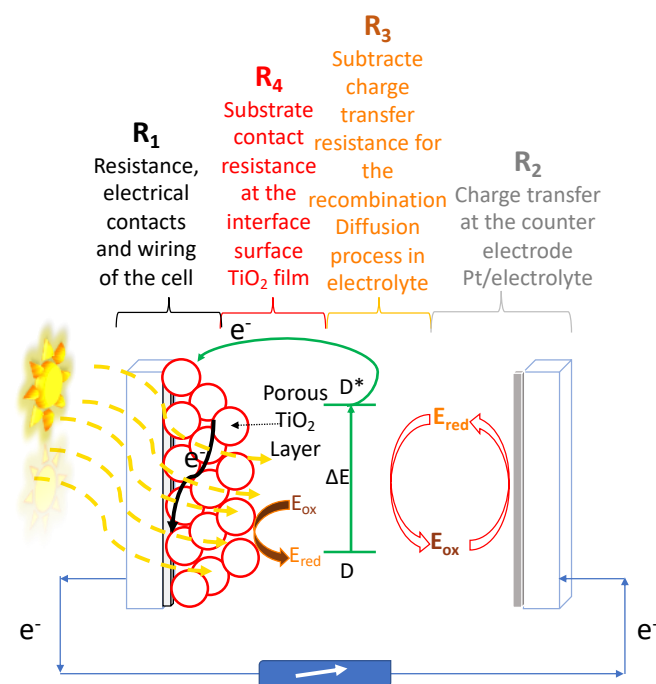
The response obtained from EIS can be represented as Nyquist plots, where the imaginary part of the impedance is plotted vs. the real part over the range of frequencies (0.01 Hz–10⁶ Hz).

Firstly, the cells were studied at different potentials in a determined range of frequencies and, then, adequate equivalent circuits have been investigated (ESI). The resistance and relaxation time (τ) obtained from the EIS data for the different eutectic mixtures (LiI:10EG, NaI:3EG, and KI:5EG) without I₂. The EIS was performed in a two-electrode symmetrical configuration cell at room temperature and applying a large variety of potentials (from 0 V or V_{OC} to ± 2.2 V).

The electrochemical process that is associated to the EIS results for the symmetrical two-electrode device could be explained by the resistance to start of the electrochemical process. Subsequently, the electrochemical charge transport or kinetics of the electron transfer, followed by the mass charge transport of the electrolyte itself, and finally followed, in some cases, by other electron transfer in the counter electrode. Taking, for example, LiI:10EG, **R1** values are almost the same for all potentials applied. This can be justify by the intrinsic resistance of the experimental apparatus. In the case of **R2** values, it decreases with the increase of the potential applied. The same behaviour is observed for **R3** values, a

decrease in the resistance with the increase of the potential. The same behaviour could be described for the others DES NaI:3EG and KI:5EG.

In order to identify the charge transfer phenomena, each different feature that is presented in the Nyquist plots could be related to the charge transfer at the counter-electrode **R2** (above 1 KHz); the electron transfer process of transport in the TiO₂ layer and the recombination **R3** (1 Hz to 1 KHz), and the diffusion into the electrolyte **R4** (<1 Hz) (Scheme 2). In the present work, the first resistance **R1** can be attributed to the material (FTO glass substrate, electrical contacts connecting to the cell, and overall apparatus).



Scheme 2. Illustration of a Dye Sensitized Solar Cell (DSSC) with the main components (Working Principles) and the kind and causes of resistances that can occur in the DSSCs.

The properties of alkali iodide based-DES plus 0.5 mol% I₂ as electrolytes have been compared with DSSCs featuring the same components (semiconducting layer, sensitizers, and electrolyte composition) and containing the reference acetonitrile/valeronitrile mixture (85:15) as an electrolyte (Table 2). Additional studies were made under illumination, in the dark and at open circuit voltage conditions (Table 2), and the properties of the sensitized TiO₂/electrolyte interface can be obtained from the Nyquist plot. The recombination processes are obtained by fitting the data with adequate equivalent circuit reported on the inset of the corresponding Figure 4.

Table 2. Resistance values obtained by fitting the electrochemical impedance spectroscopy data in a determined frequency range for the different prepared eutectic mixtures at selected potential for the prepared DSSCs using eutectic mixtures plus I₂ as electrolyte.

Electrolyte	Potential [(V)]	Resistance ($\Omega \cdot \text{cm}^2$)			
		R1	R4	R3	R2
Reference	SUN	3.31	1.55	2.04	-
	DARK (−425 mV)	3.35	5.85	0.587	-
	DARK (425 mV)	3.32	1.79	8.95	-

Table 2. Cont.

Electrolyte	Potential [(V)]	Resistance ($\Omega \cdot \text{cm}^2$)			
		R1	R4	R3	R2
KI:5EG + 0.5 mol% I ₂	SUN	3.14	1.00	2.94	1.52
	DARK (−500 mV)	2.70	16.26	123.34	69.93
	DARK (500 mV)	3.27	1.49	4.12	2.87
LiI:10EG + 0.5 mol% I ₂	SUN	3.36	2.20	1.68	2.20
	DARK (−500 mV)	3.38	5.13	2.14	2.78
	DARK (500 mV)	3.37	2.08	2.65	5.40

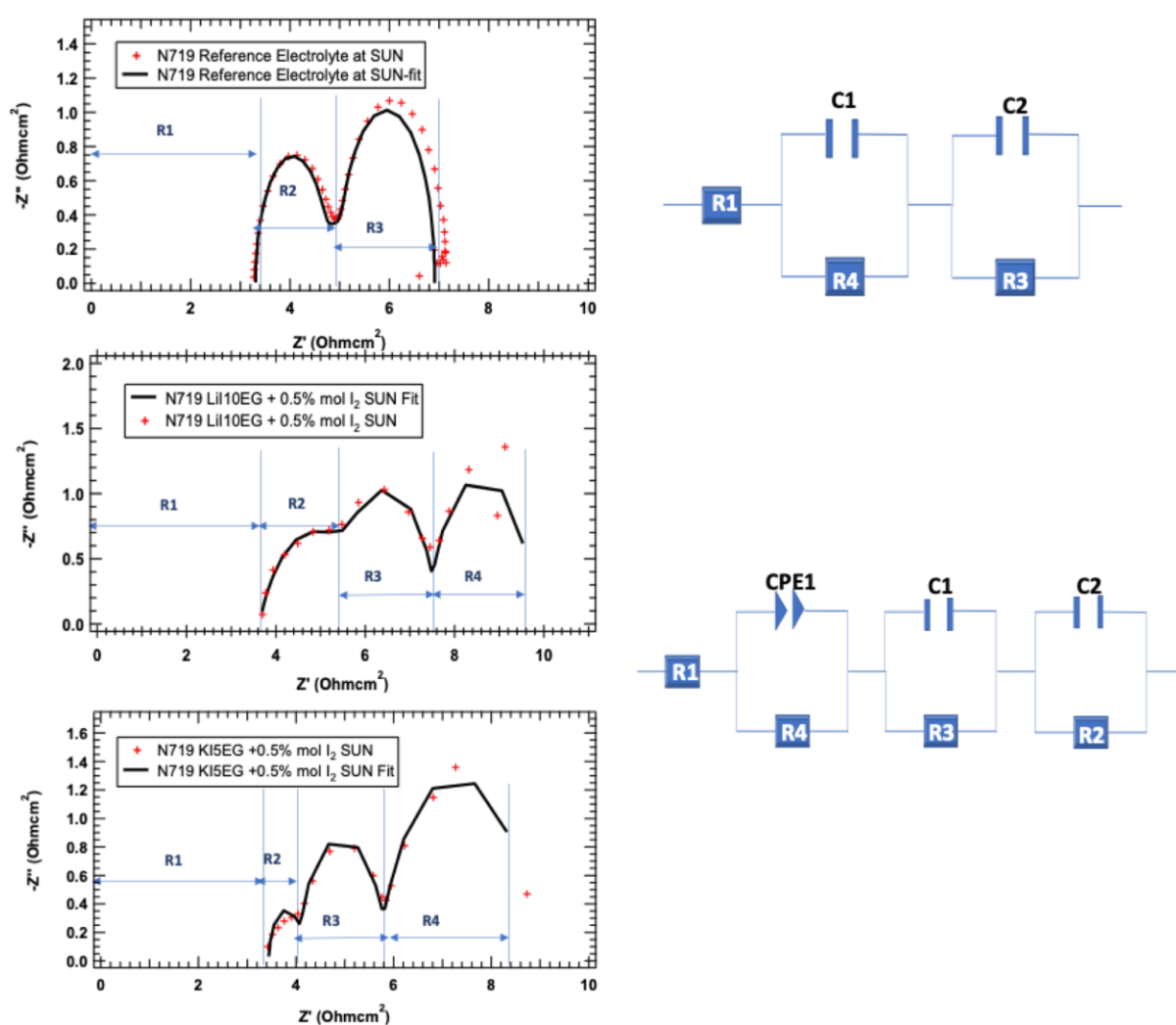


Figure 4. Nyquist plots of Reference (**top**) LiI:10EG + 0.5 mol% I₂ (**middle**) and KI:5EG + 0.5 mol% I₂ (**bottom**) accompanied with the respective fitting and equivalent circuit under illumination.

From Figure 4, it can be observed that, for the iodide based-eutectic solvents plus 0.5 mol% of I₂ electrolyte under illumination at 1 SUN, and the results can be described, as follows:

- (1) In the case of **R1**, the resistance that can be attributed to the materials used, including cables, is almost the same for all electrolytes studied, i.e., the electrolyte does not influence this parameter.

- (2) **R2**, (above 1 KHz) is related with the resistance to the charge transfer at counter electrode (Pt/electrolyte) interface and redox couple regeneration at the counter-electrode. This phenomenon can be observed in Figure 4, and the following trend for the electrolytes studied was verified: KI:5EG + 0.5 mol% I₂ < Reference < LiI:10EG + 0.5 mol% I₂. This could be related to the bulkier K⁺ cation. The cation bulkier radius allows lower resistance to the regeneration of the redox couple. While Li⁺, a smaller cation, can be more easily found in the vicinity of the electrode and the redox pair stabilizing them, thus increasing the resistance to the regeneration process. This is even more significant in the presence of the EG.
- (3) **R3** (1 Hz to 1 KHz), associated to the electron transfer process (transport) in the TiO₂ layer, the recombination and dye regeneration, LiI:10EG + 0.5 mol% I₂ < Reference < KI:5EG + 0.5 mol% I₂. In this case, the DES LiI:10EG + 0.5 mol% I₂ allows a faster regeneration of the dye, probably due to the amount of Li⁺ cation that can intercalate with the dye/TiO₂ nanomaterial, even when comparing with Reference (lower amounts of Li⁺). Moreover, in the presence of high concentrations of EG, a strong interaction between Li⁺:EG might be occurring, leaving the redox pair more available for dye regeneration. The bulkier K⁺ cation could act as an umbrella, lowering the intercalation process and, consequently, the number of photo-injected electrons on the TiO₂ nanomaterial when compared with the Li⁺ cation, as expected.
- (4) **R4** (<1 Hz), is related to the diffusion of the species into the electrolyte. This particular process and, as expected for a well-studied Reference electrolyte, is so fast that it is not observed in terms of resistance to the process, as in Table 2. This electrolyte allows for a fast diffusion of the species, as can be seen from Figure 4. In the case of the DES based electrolyte KI:5EG + 0.5 mol% I₂ < LiI:10EG + 0.5 mol% I₂, some unexpected results were obtained. The bulkier K⁺ cation allows for a better diffusion process than the Li⁺, a smaller cation in the presence of EG, although being the same cation used in the reference (which presents no resistance to the diffusion process). Additionally, increasing the amount of EG from K⁺ to Li⁺ should lower the viscosity, thus increasing the diffusion process, which is the opposite of what was experimentally observed. This could be related with the formation of LiI:10EG + 0.5 mol% I₂ by the self-complexation (Hydrogen bonds (HB) between the iodide and the alcohol of the Ethylene Glycol) leaving the Li⁺ relatively free. R4 (<1 Hz) is related to the diffusion of the species into the electrolyte. This particular process and, as expected for a well-studied Reference electrolyte, is so fast that it is not observed in terms of resistance to the process, as shown in Table 2. This electrolyte allows for a fast diffusion of the species, as can be seen from Figure 4. In the case of the DES based electrolyte KI:5EG + 0.5 mol% I₂ < LiI:10EG + 0.5 mol% I₂ some unexpected results were obtained. The bulkier K⁺ cation allows a better diffusion process than when the Li⁺, a smaller cation in the presence of EG, despite being the same cation used in the reference (which presents no resistance to the diffusion process). Additionally, increasing the amount of EG from K⁺ to Li⁺ should lower the viscosity thus increasing the diffusion process, which is the opposite of what was experimentally observed. This could be related with the formation of LiI:10EG + 0.5 mol% I₂ by the self-complexation (Hydrogen bonds [HB] between the iodide and the alcohol of the Ethylene Glycol) leaving the Li⁺ relatively free.

R4 is the regeneration of the redox pair I⁻/I₃⁻ and **R3** is associated to the electron transfer process, a hypothetical explanation for these resistive processes is the possibility that the K⁺ moves faster than the Li⁺ in an ocean of I⁻/I₃⁻ anions. Despite being a bulkier cation, K⁺ stays further from the I⁻/I₃⁻ free and self-complexed by HB with the alcohol of the Ethylene Glycol. Because Li⁺ interacts strongly (highest charge density) with the I⁻/I₃⁻ free and self-complexed by HB with the alcohol of the Ethylene Glycol, it remains less available to move freely and intercalate with the dye/TiO₂ nanomaterial.

Finally, for the case of DSSCs studies subjected to illumination, lower values of the resistance to the transfer process. The best performance of the cell is expected. In this study: for the interface redox/counter electrode, the best result is obtained for KI:5EG + 0.5 mol%

I_2 , for the dye regeneration is the LiI:10EG + 0.5 mol% I_2 , and for the diffusion process is the reference. However, overall, the reference is the best performing electrolyte followed by the KI:5EG + 0.5 mol% I_2 , and, finally, LiI:10EG + 0.5 mol% I_2 .

In the dark, under forward bias, a smaller resistance indicates a faster charge recombination, therefore a larger dark current and a lower device voltage. This parameter is key for the maximum performance that is attainable by the cell, because the recombination resistance controls in what way the generated charge might be lost [49]. The interface phenomena seen in the DES-based DSSCs and reference devices could be extensively distinctive, as can be seen in Table 2.

In Figure 5, for a better comparison between the results obtained for the reference DSSC and the DES + 0.5 mol% I_2 : (a) applying potentials of 0.43 or 0.5 V in the dark, where the regeneration of the redox couple is studied; from our viewpoint, the lowest the resistance values leads to a better regeneration of the redox couple and some trends can be observed: **R1** is fairly the same in all cases; **R4** is lower in the case of KI:5EG + 0.5 mol% I_2 , followed by the Reference, and the highest is the LiI:10EG + 0.5 mol% I_2 ; **R3** is highest for the Reference, followed by KI:5EG + 0.5 mol% I_2 , and finally LiI:10EG + 0.5 mol% I_2 ; and, for **R2**, no result was obtained for the Reference, the process is too fast, and it is higher for LiI:10EG + 0.5 mol% I_2 than for KI:5EG + 0.5 mol% I_2 ; (b) in the dark applying -0.43 or -0.5 V, where the dye regeneration/ TiO_2 is studied; the higher the resistance to the process the better, since there is less probability of recombination taking place, hence reflecting longer recombination times. A similar behaviour could be described: **R1** is fairly the same in all cases; **R4** is lower in the case of LiI:10EG + 0.5 mol% I_2 , followed by the Reference and the highest is KI:5EG + 0.5 mol% I_2 that is 3x higher; **R3** is highest for KI:5EG + 0.5 mol% I_2 , almost 25x higher than LiI:10EG + 0.5 mol% I_2 and 200x higher than the Reference; and, **R2** for KI:5EG + 0.5 mol% I_2 is almost 25x higher than for LiI:10EG + 0.5 mol% I_2 , no resistance is observed for the Reference.

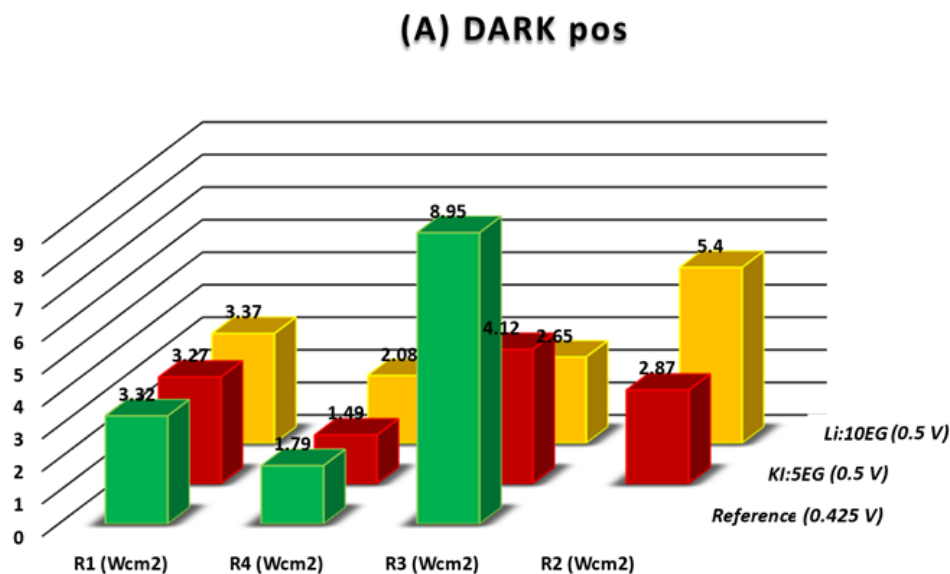


Figure 5. Cont.

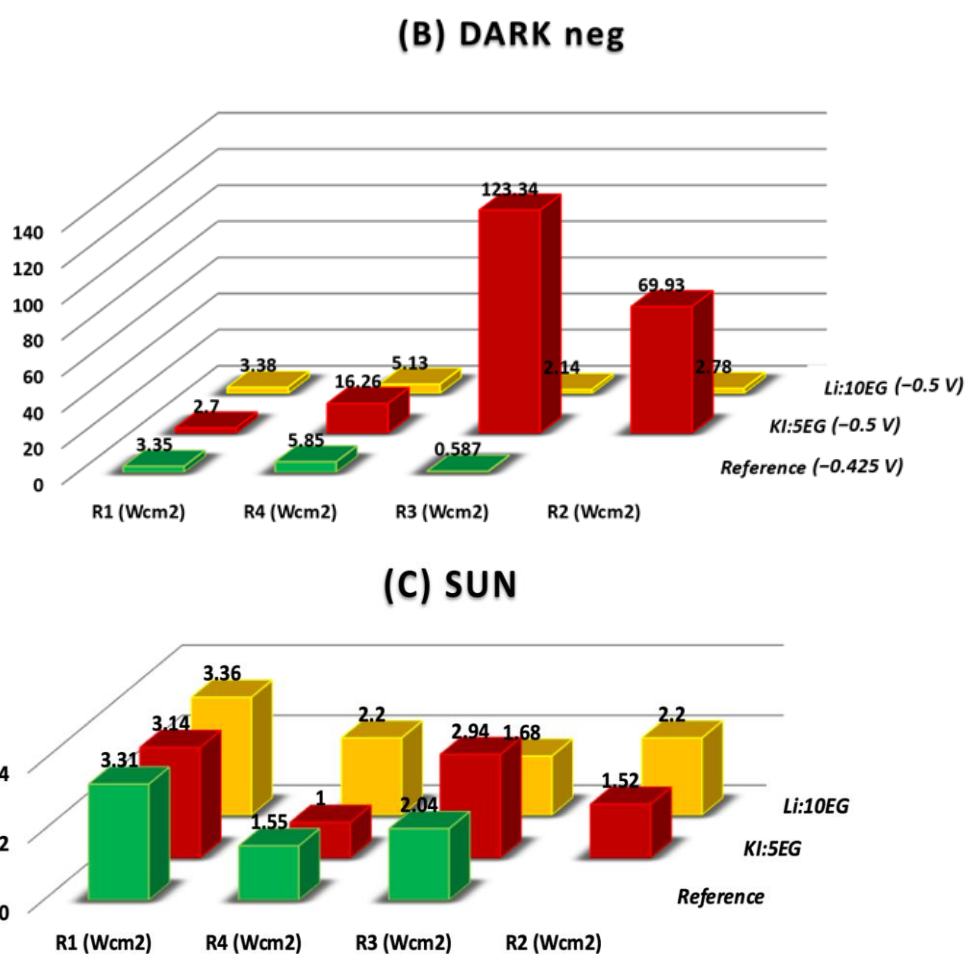


Figure 5. Resistance values obtained for the different alkali iodides based-DES plus 0.5 mol % I₂ incorporated as electrolyte for DSSCs. Legend: (A) DARK pos; (B) DARK neg; and, (C) SUN.

Finally, since, under illumination, the lower overall resistance the better, it can be observed that the reference presents the lower overall resistance to all of the processes involved in the DSSC, allowing it to have the highest efficiency and highest current density. The best performing DES-based electrolyte was KI:5EG + 0.5 mol% I₂, presenting a relatively good efficiency, half the value obtained for the reference, which is due to increased dye recombination and diffusion processes in the electrolyte (R₃ and R₂, respectively). Despite having the same cation as the Reference electrolyte, LiI:10EG + 0.5 mol% I₂ was the worst performing electrolyte in the EIS studies.

3. Experimental

3.1. Chemicals

All of the commercially available reactants were of high purity and they were used without further purification and stored under inert conditions. Glycerol (Gly) and Poly(ethylene glycol) derivatives (PEG 200, 400) were purchased from Sigma- Aldrich (Munich, Germany) (Reagent Plus, 99% GC), Ethylene Glycol (EG) from Alfa Aesar (Heysham, UK) (99%). The HBD chemical reagents LiI, LiI·xH₂O from Sigma-Aldrich (crystalline powder 99.9% trace metal basis and purum > 98%, respectively) KI from Merck (Kenilworth, NJ, USA) and NaI from Alfa Aesar 99+% dry wt water.

3.2. Synthesis of DES

The ESs were prepared using iodide derivatives as HBA, such as LiI, LiI·xH₂O, NaI·xH₂O, KI·xH₂O, and as HBD Ethylene Glycol (EG), Glycerol (Gly), and poly(ethylene

glycol) 200 and 400 (PEG 200 and PEG 400) in adequate proportion, temperature between 50–80 °C, with stirring until a homogenous liquid was obtained [3–5].

3.3. Electrochemical Measurements

3-electrode Configuration Cyclic Voltammetry

The group already published the CV experiments elsewhere [50].

3.4. Electrochemical Impedance Spectroscopy (EIS)

In the two-electrode configuration cell (area of electroactive surface is $2 \times 1 \text{ cm}^2$), the conductive layers were rinsed with ethanol. EIS applying a controlled potential from 0 V to 2.2 V vs. Open circuit potential (OCP) with a step potential of 0.1 V in an Autolab PGSTAT 12 potentiostat/galvanostat, controlled with GPES/FRA2 software version 4.9 (Eco-Chemie, B.V. Software, Utrecht in the Netherlands) allowing for the characterization of the DES material.

3.5. DSSCs Fabrication and Photovoltaic Characterization

The procedure was followed, as described elsewhere. Ref. [51] The conductive FTO-glass (TEC7, Greatcell Solar, Queanbeyan, Australia) used for the preparation of the transparent electrodes was first cleaned with detergent and then washed with water and ethanol. To prepare the anodes, the conductive glass plates (area: $15 \text{ cm} \times 4 \text{ cm}$) were immersed in a TiCl_4 /water solution (40 mM) at 70 °C for 30 min., washed with water and ethanol, and then sintered at 500 °C for 30 min. This procedure is essential in order to improve the adherence of the following deposited nanocrystalline layers to the glass plates, as well as to behave as a 'blocking-layer', helping to block charge recombination between electrons in the FTO with holes in the I^-/I_3^- redox couple. Afterwards, the TiO_2 nanocrystalline layers were deposited on these pre-treated FTO plates by screen-printing the transparent titania paste (18NR-T, Greatcell Solar) using a frame with polyester fibres having 43.80 mesh per cm^2 . This procedure, involving two steps (coating and drying at 125 °C), was repeated two times. The TiO_2 coated plates were gradually heated up to 325 °C, the temperature was increased to 375 °C in 5 min, and then afterwards to 500 °C. The plates were sintered at this temperature for 30 min., and finally cooled down to room temperature. A second treatment with the same TiCl_4 /water solution (40 mM) was performed, following the previously described procedure. This second TiCl_4 treatment is also an optimization step. It will enhance the surface roughness for dye adsorption, thus positively affecting the photocurrent produced by the cell under illumination. Finally, a coating of reflector titania paste (WER2-O, Greatcell Solar) was deposited by screen-printing and sintered at 500 °C. This layer of 150–200 nm sized anatase particles is used to function as a 'photon-trapping' layer, also to improve photocurrent. Each anode was cut into rectangular pieces (area: $2 \text{ cm} \times 1.5 \text{ cm}$), having a spot area of 0.196 cm^2 with a thickness of 15 μm . The prepared anodes were soaked for 2 h in a 0.5 mM N719 ethanol solution, at room temperature in the dark. The excess dye was removed by rinsing the photoanodes with ethanol.

Each counter-electrode consisted of an FTO-glass plate (area: $2 \text{ cm} \times 2 \text{ cm}$), on which a hole (1.5 mm diameter) was drilled. The perforated substrates were washed and cleaned with water and ethanol in order to remove any residual glass powder and organic contaminants. The Pt transparent catalyst (PT1, Greatcell Solar) was deposited on the conductive face of the FTO-glass by doctor blade: one edge of the glass plate was covered with a stripe of an adhesive tape (3 M Magic) to both control the thickness of the film and mask an electric contact strip. The Pt paste was spread uniformly on the substrate by sliding a glass rod along the tape spacer. The adhesive tape stripe was removed, and the glasses heated at 550 °C for 30 min. The photoanode and the Pt counter-electrode were assembled into a sandwich type arrangement and sealed (using a thermopress) with a hot melt gasket that was made of Surlyn ionomer (Meltonix 1170-25, Solaronix SA, Aubonne, Switzerland).

The 'Reference' electrolyte was prepared by dissolving the redox couple, I^-/I_2 (0.8 M LiI and 0.05 M I_2), in acetonitrile/valeronitrile (85:15, % v/v) mixture. All of the studied

electrolytes were introduced into the cell via backfilling under vacuum through the drilled hole in the back of the cathode. Finally, the hole was sealed with adhesive tape.

3.6. Photoelectrochemical Measurements

Current–Voltage curves were recorded by a digital Keithley SourceMeter multimeter (PVIV-1A) that was connected to a PC. Simulated sunlight irradiation was provided by an Oriel solar simulator (Model LCS-100 Small Area Sol1A, 300 W Xe Arc lamp equipped with AM 1.5 filter, 100 mW/cm²). The thickness of the oxide film deposited on the photoanodes was measured using an Alpha-Step D600 Stylus Profiler (KLA-Tencor, Milpitas, CA, USA).

4. Conclusions

Different alkali iodide based deep eutectic solvents (DES) that were composed by LiI:nEG, NaI:nEG, and KI:nEG as electrolytes for dye sensitized solar cells (DSSCs) have been explored. Different amounts of iodine (I₂) were added to original DES electrolyte in order to improve their electrolyte performance. The cation effect on DSSC performance was studied for electrolytes-based on DES-alkali metal (LiI, NaI, KI). As expected, the open-circuit voltage (V_{OC}) increased with the increase in cation radius from Li⁺ to K⁺ when illuminated. However, the expected trade-off phenomenon between V_{OC} and J_{SC} was not verified. The cation effect strongly depends on the cation density in the electrolyte and the adsorption ability on the TiO₂. Li⁺ is known to intercalate into the TiO₂ lattice, and its effect on the short-circuit current and open circuit voltage is described to be more remarkable when present in high concentration in the electrolyte. DES can be promising, since they present higher V_{OC} (up to 140 mV), similar FF values, but less current density values, when compared with a reference electrolyte in the same experimental conditions. Electrochemical impedance spectroscopy (EIS) studies revealed a correlation between the resistive processes taking place in the devices and the lower performances verified for the DES-based cells. The DSSC using the electrolyte KI:5EG + 0.5 mol% of I₂ presents a J_{SC} of 6.05 mA/cm² and V_{OC} of 0.545 V. Furthermore, its efficiency decreased by only 60% after seven months of operation. With no further addition of fresh electrolyte or dye, a performance of J_{SC} 2 mA/cm² and V_{OC} 0.4 V was obtained. After optimization of the DES electrolytes, they could present a good alternative to the volatile organic compounds (VOC)-based electrolytes used in these DSSCs.

Author Contributions: Conceptualization, H.C. and L.C.B.; Formal analysis, A.L.P. and L.A.N.; methodology, H.C. and N.J.; investigation, H.C., A.L.P., N.J. and L.C.B.; writing—original draft preparation, H.C., N.J. and L.C.B.; writing—review and editing, A.L.P., L.A.N. and L.C.B.; supervision, L.C.B.; funding acquisition, L.C.B. All authors have read and agreed to the published version of the manuscript.

Funding: This work was supported by Fundação para a Ciência e Tecnologia (FCT, Portugal) through national funds (PTDC/QEQ-QFI/1971/2014) and the project “SunStorage: Harvesting and storage of solar energy”, with reference POCI- 01-0145-FEDER-016387, funded by European Regional Development Fund (ERDF), through COMPETE 2020-Operational Programme for REQUIMTE, which is financed by the Portuguese FCT/MCTES (UID/QUI/50006/2019). The authors would like to thanks to Professor Madalena Dionisio and Professor João C. Lima for fruitful discussions.

Institutional Review Board Statement: Not applicable.

Informed Consent Statement: Not applicable.

Data Availability Statement: Not applicable.

Acknowledgments: Hugo Cruz thanks to Fundação para a Ciência e a Tecnologia, MCTES, for the Norma transitória DL 57/2016 Program Contract. Luísa A. Neves thanks—FCT Investigator Contract (IF/00505/2014). Ana Lucia Pinto thanks for the Grant PD/BD/135087/2017.

Conflicts of Interest: The authors declare no conflict of interest.

References

1. Armaroli, N.; Balzani, V. Solar Electricity and Solar Fuels: Status and Perspectives in the Context of the Energy Transition. *Chem. A Eur. J.* **2016**, *22*, 32–57. [[CrossRef](#)] [[PubMed](#)]
2. Su'Ait, M.; Rahman, M.; Ahmad, A. Review on polymer electrolyte in dye-sensitized solar cells (DSSCs). *Sol. Energy* **2015**, *115*, 452–470. [[CrossRef](#)]
3. Susanti, D.; Nafi, M.; Purwaningsih, H.; Fajarin, R.; Kusuma, G.E. The Preparation of Dye Sensitized Solar Cell (DSSC) from TiO₂ and Tamarillo Extract. *Procedia Chem.* **2014**, *9*, 3–10. [[CrossRef](#)]
4. O'Regan, B.; Grätzel, M.; Gr, M. A low-cost, high-efficiency solar cell based on dye-sensitized colloidal TiO₂ films. *Nature* **1991**, *353*, 737–740. [[CrossRef](#)]
5. Hagberg, D.P.; Yum, J.-H.; Lee, H.; De Angelis, F.; Marinado, T.; Karlsson, K.M.; Humphry-Baker, R.; Sun, L.; Hagfeldt, A.; Grätzel, M.; et al. Molecular Engineering of Organic Sensitizers for Dye-Sensitized Solar Cell Applications. *J. Am. Chem. Soc.* **2008**, *130*, 6259–6266. [[CrossRef](#)] [[PubMed](#)]
6. Grätzel, M. Photoelectrochemical cells. *Nature* **2001**, *414*, 338–344. [[CrossRef](#)] [[PubMed](#)]
7. Grätzel, M. Solar Energy Conversion by Dye-Sensitized Photovoltaic Cells. *Inorg. Chem.* **2005**, *44*, 6841–6851. [[CrossRef](#)] [[PubMed](#)]
8. Nazeeruddin, M.K.; Liska, P.; Moser, J.; Vlachopoulos, N.; Grätzel, M. Conversion of Light into Electricity with Trinuclear Ru-thenium Complexes Adsorbed on Textured TiO₂ Film. *Helv. Chim. Acta* **1990**, *73*, 1788–1803. [[CrossRef](#)]
9. Wang, Q.; Moser, A.J.-E.; Grätzel, M. Electrochemical Impedance Spectroscopic Analysis of Dye-Sensitized Solar Cells. *J. Phys. Chem. B* **2005**, *109*, 14945–14953. [[CrossRef](#)]
10. Higashino, T.; Imahori, H. Porphyrins as excellent dyes for dye-sensitized solar cells: Recent developments and insights. *Dalton Trans.* **2014**, *44*, 448–463. [[CrossRef](#)]
11. Kay, A.; Graetzel, M. Artificial photosynthesis. 1. Photosensitization of titania solar cells with chlorophyll derivatives and related natural porphyrins. *J. Phys. Chem.* **1993**, *97*, 6272–6277. [[CrossRef](#)]
12. Campbell, W.M.; Jolley, K.W.; Wagner, P.; Wagner, K.; Walsh, P.J.; Gordon, K.C.; Schmidt-Mende, L.; Nazeeruddin, M.K.; Wang, Q.; Grätzel, M.; et al. Highly Efficient Porphyrin Sensitizers for Dye-Sensitized Solar Cells. *J. Phys. Chem. C* **2007**, *111*, 11760–11762. [[CrossRef](#)]
13. Cherepy, N.J.; Smestad, G.P.; Grätzel, A.M.; Zhang, J.Z. Ultrafast Electron Injection: Implications for a Photoelectrochemical Cell Utilizing an Anthocyanin Dye-Sensitized TiO₂ Nanocrystalline Electrode. *J. Phys. Chem. B* **1997**, *101*, 9342–9351. [[CrossRef](#)]
14. Calogero, G.; Di Marco, G.; Caramori, S.; Cazzanti, S.; Argazzi, R.; Bignozzi, C.A. Natural dye sensitizers for photoelectrochemical cells. *Energy Environ. Sci.* **2009**, *2*, 1162–1172. [[CrossRef](#)]
15. Calogero, G.; Yum, J.-H.; Sinopoli, A.; Di Marco, G.; Grätzel, M.; Nazeeruddin, M.K. Anthocyanins and betalains as light-harvesting pigments for dye-sensitized solar cells. *Sol. Energy* **2012**, *86*, 1563–1575. [[CrossRef](#)]
16. Calogero, G.; Sinopoli, A.; Citro, I.; Di Marco, G.; Petrov, V.; Diniz, A.M.; Parola, A.J.; Pina, F. Synthetic analogues of anthocyanins as sensitizers for dye-sensitized solar cells. *Photochem. Photobiol. Sci.* **2013**, *12*, 883–894. [[CrossRef](#)]
17. Calogero, G.; Bartolotta, A.; Di Marco, G.; Di Carlo, A.; Bonaccorso, F. Vegetable-based dye-sensitized solar cells. *Chem. Soc. Rev.* **2015**, *44*, 3244–3294. [[CrossRef](#)]
18. Pinto, A.L.; Cruz, L.; Gomes, V.; Cruz, H.; Calogero, G.; De Freitas, V.; Pina, F.; Parola, A.J.; Lima, J.C. Catechol versus carboxyl linkage impact on DSSC performance of synthetic pyranoflavylum salts. *Dye. Pigment.* **2019**, *170*, 107577. [[CrossRef](#)]
19. Santra, P.K.; Kamat, P.V. Mn-Doped Quantum Dot Sensitized Solar Cells: A Strategy to Boost Efficiency over 5%. *J. Am. Chem. Soc.* **2012**, *134*, 2508–2511. [[CrossRef](#)]
20. Jeon, N.J.; Noh, J.H.; Yang, W.S.; Kim, Y.C.; Ryu, S.; Seo, J.; Seok, S.I. Compositional engineering of perovskite materials for high-performance solar cells. *Nat. Cell Biol.* **2015**, *517*, 476–480. [[CrossRef](#)] [[PubMed](#)]
21. Gao, P.; Grätzel, M.; Nazeeruddin, M.K. Organohalide lead perovskites for photovoltaic applications. *Energy Environ. Sci.* **2014**, *7*, 2448–2463. [[CrossRef](#)]
22. He, M.; Zheng, D.; Wang, M.; Lin, C.; Lin, Z. High efficiency perovskite solar cells: From complex nanostructure to planar heterojunction. *J. Mater. Chem. A* **2014**, *2*, 5994–6003. [[CrossRef](#)]
23. Law, C.; Pathirana, S.C.; Li, X.; Anderson, A.Y.; Barnes, P.R.F.; Listorti, A.; Ghaddar, T.H.; O'regan, B.C. Water-Based Electrolytes for Dye-Sensitized Solar Cells. *Adv. Mater.* **2010**, *22*, 4505–4509. [[CrossRef](#)]
24. Mahmood, A. Recent research progress on quasi-solid-state electrolytes for dye-sensitized solar cells. *J. Energy Chem.* **2015**, *24*, 686–692. [[CrossRef](#)]
25. Mishra, A.; Fischer, M.K.R.; Bäuerle, P. Metal-Free Organic Dyes for Dye-Sensitized Solar Cells: From Structure: Property Relationships to Design Rules. *Angew. Chem. Int. Ed.* **2009**, *48*, 2474–2499. [[CrossRef](#)] [[PubMed](#)]
26. Abbott, A.P.; Capper, G.; Davies, D.L.; Rasheed, R.K. Ionic Liquid Analogues Formed from Hydrated Metal Salts. *Chem. A Eur. J.* **2004**, *10*, 3769–3774. [[CrossRef](#)] [[PubMed](#)]
27. Smith, E.L.; Abbott, A.P.; Ryder, K.S. Deep Eutectic Solvents (DESs) and Their Applications. *Chem. Rev.* **2014**, *114*, 11060–11082. [[CrossRef](#)]
28. Yang, Q.; Zhang, Z.; Sun, X.-G.; Hu, Y.-S.; Xing, H.; Dai, S. Ionic liquids and derived materials for lithium and sodium batteries. *Chem. Soc. Rev.* **2018**, *47*, 2020–2064. [[CrossRef](#)] [[PubMed](#)]
29. Sakita, A.M.P.; Della Noce, R.; Fugivara, C.S.; Benedetti, A.V. On the cobalt and cobalt oxide electrodeposition from a glyceline deep eutectic solvent. *Phys. Chem. Chem. Phys.* **2016**, *18*, 25048–25057. [[CrossRef](#)] [[PubMed](#)]

30. Miller, M.A.; Wainright, J.S.; Savinell, R.F. Iron Electrodeposition in a Deep Eutectic Solvent for Flow Batteries. *J. Electrochem. Soc.* **2017**, *164*, A796–A803. [[CrossRef](#)]
31. Mondal, D.; Sharma, M.; Wang, C.-H.; Lin, Y.-C.; Huang, H.-C.; Saha, A.; Nataraj, S.K.; Prasad, K. Deep eutectic solvent promoted one step sustainable conversion of fresh seaweed biomass to functionalized graphene as a potential electrocatalyst. *Green Chem.* **2016**, *18*, 2819–2826. [[CrossRef](#)]
32. Bhatt, J.; Mondal, D.; Bhojani, G.; Chatterjee, S.; Prasad, K. Preparation of bio-deep eutectic solvent triggered cephalopod shaped silver chloride-DNA hybrid material having antibacterial and bactericidal activity. *Mater. Sci. Eng. C* **2015**, *56*, 125–131. [[CrossRef](#)] [[PubMed](#)]
33. Mukesh, C.; Gupta, R.; Srivastava, D.N.; Nataraj, S.K.; Prasad, K. Preparation of a natural deep eutectic solvent mediated self polymerized highly flexible transparent gel having super capacitive behaviour. *RSC Adv.* **2016**, *6*, 28586–28592. [[CrossRef](#)]
34. Chakrabarti, M.H.; Mjalli, F.S.; AlNashef, I.M.; Hashim, M.A.; Hussain, M.A.; Bahadori, L.; Low, C.T.J. Prospects of applying ionic liquids and deep eutectic solvents for renewable energy storage by means of redox flow batteries. *Renew. Sustain. Energy Rev.* **2014**, *30*, 254–270. [[CrossRef](#)]
35. Zhang, C.; Ding, Y.; Zhang, L.; Wang, X.; Zhao, Y.; Zhang, X.; Yu, G. A Sustainable Redox-Flow Battery with an Aluminum-Based, Deep-Eutectic-Solvent Anolyte. *Angew. Chem. Int. Ed.* **2017**, *56*, 7454–7459. [[CrossRef](#)] [[PubMed](#)]
36. Liu, P.; Hao, J.-W.; Mo, L.-P.; Zhang, Z.-H. Recent advances in the application of deep eutectic solvents as sustainable media as well as catalysts in organic reactions. *RSC Adv.* **2015**, *5*, 48675–48704. [[CrossRef](#)]
37. Parnham, E.R.; Morris, R.E. Ionothermal Synthesis of Zeolites, Metal–Organic Frameworks, and Inorganic–Organic Hybrids. *Accounts Chem. Res.* **2007**, *40*, 1005–1013. [[CrossRef](#)] [[PubMed](#)]
38. Carriazo, D.; Serrano, M.C.; Gutiérrez, M.C.; Ferrer, M.L.; Del Monte, F. Deep-eutectic solvents playing multiple roles in the synthesis of polymers and related materials. *Chem. Soc. Rev.* **2012**, *41*, 4996–5014. [[CrossRef](#)] [[PubMed](#)]
39. Cruz, H.; Jordão, N.; Branco, L.C. Deep eutectic solvents (DESs) as low-cost and green electrolytes for electrochromic devices. *Green Chem.* **2017**, *19*, 1653–1658. [[CrossRef](#)]
40. Cruz, H.; Jordão, N.; Amorim, P.; Dionísio, M.; Branco, L.C. Deep Eutectic Solvents as Suitable Electrolytes for Electrochromic Devices. *ACS Sustain. Chem. Eng.* **2017**, *6*, 2240–2249. [[CrossRef](#)]
41. Jordão, N.; Cruz, H.; Pina, F.; Branco, L.C. Studies of bipyridinium ionic liquids and deep eutectic solvents as electrolytes for electrochromic devices. *Electrochim. Acta* **2018**, *283*, 718–726. [[CrossRef](#)]
42. Cruz, H.; Jordão, N.; Dionísio, M.; Pina, F.; Branco, L.C. Intrinsically Electrochromic Deep Eutectic Solvents. *ChemistrySelect* **2019**, *4*, 1530–1534. [[CrossRef](#)]
43. Jhong, H.-R.; Wong, D.S.-H.; Wan, C.-C.; Wang, Y.-Y.; Wei, T.-C. A novel deep eutectic solvent-based ionic liquid used as electrolyte for dye-sensitized solar cells. *Electrochem. Commun.* **2009**, *11*, 209–211. [[CrossRef](#)]
44. Boldrini, C.L.; Manfredi, N.; Perna, F.M.; Trifiletti, V.; Capriati, V.; Abboto, A. Dye-Sensitized Solar Cells that use an Aqueous Choline Chloride-Based Deep Eutectic Solvent as Effective Electrolyte Solution. *Energy Technol.* **2017**, *5*, 345–353. [[CrossRef](#)]
45. Boldrini, C.L.; Manfredi, N.; Perna, F.M.; Capriati, V.; Abboto, A. Designing Eco-Sustainable Dye-Sensitized Solar Cells by the Use of a Menthol-Based Hydrophobic Eutectic Solvent as an Effective Electrolyte Medium. *Chem. Eur. J.* **2018**, *24*, 17656–17659. [[CrossRef](#)] [[PubMed](#)]
46. Boldrini, C.L.; Manfredi, N.; Perna, F.M.; Capriati, V.; Abboto, A. Eco-Friendly Sugar-Based Natural Deep Eutectic Solvents as Effective Electrolyte Solutions for Dye-Sensitized Solar Cells. *ChemElectroChem* **2020**, *7*, 1707–1712. [[CrossRef](#)]
47. Jennings, J.R.; Wang, Q. Influence of Lithium Ion Concentration on Electron Injection, Transport, and Recombination in Dye-Sensitized Solar Cells. *J. Phys. Chem. C* **2009**, *114*, 1715–1724. [[CrossRef](#)]
48. Jiang, K.; Yanagida, S. Optimization of Redox Mediators and Electrolytes. In *Dye-Sensitized Solar Cells*; Kalyanasundaram, K., Ed.; EPFL Press: Lausanne, Switzerland, 2010; p. 117.
49. Barnes, P.R.F.; Anderson, A.Y.; Juozapavicius, M.; Liu, L.; Liu, X.; Palomares, E.; Forneli, A.; O'Regan, B.C. Factors controlling charge recombination under dark and light conditions in dye sensitised solar cells. *Phys. Chem. Chem. Phys.* **2011**, *13*, 3547. [[CrossRef](#)]
50. Cruz, H.; Jordao, N.; Pinto, A.L.; Dionísio, M.; Neves, L.A.; Branco, L.C. Alkaline Iodide-Based Deep Eutectic Solvents for Electrochemical Applications. *ACS Sustain. Chem. Eng.* **2020**, *8*, 10653–10663. [[CrossRef](#)]
51. Cruz, H.; Pinto, A.L.; Lima, J.C.; Branco, L.C.; Gago, S. Application of polyoxometalate-ionic liquids (POM-ILs) in dye-sensitized solar cells (DSSCs). *Mater. Lett. X* **2020**, *6*, 100033. [[CrossRef](#)]